Talanta 82 (2010) 1218–1224

Contents lists available at ScienceDirect

Talanta

journal homepage: www.elsevier.com/locate/talanta

A novel electrochemical sensor based on nano-structured film electrode for monitoring nitric oxide in living tissues

Xiaocui Deng, Fang Wang, Zilin Chen*

Institute of Pharmaceutical Analysis, College of pharmacy, Wuhan University, Donghu Road No 185, Wuhan 430071, China

ARTICLE INFO

Article history:
Received 20 March 2010
Received in revised form 22 June 2010
Accepted 24 June 2010
Available online 3 July 2010

Keywords:
Nitric oxide sensor
Multi-walled carbon nanotube
Gold nanoparticle
Nitroglycerin
Aspirin

ABSTRACT

A sensor exhibited high sensitivity and good selectivity for determination of nitric oxide (NO) was fabricated. The sensor was constructured by coating Nafion/multi-walled carbon nanoubes-chitosan-gold nanoparticles (Nafion/MWNTs-CS-AuNPs) film on glassy carbon electrode (GCE). Several key parameters affecting on the electrochemical response were optimized, such as the film thickness, applied potential and volume of Nafion. The sensor showed good linear relationship with the NO concentration in the range of 1.90×10^{-8} to 5.40×10^{-5} M and with the detection limit of 7.60×10^{-9} M ($S/N = 3$). Finally, the sensor was successfully applied to the monitoring of NO release from living tissues, including mouse kidney, heart, spleen and liver (a slice). NO release at micro-molar level can be detected while the NO donor L-arginine (L-Arg), nitroglycerin (GTN) and aspirin (ASA) was present. It was interestedly found that the capacities to induce NO generation were in the order of GTN > ASA > L-Arg when these stimulants were converted to the same concentration. In addition, the NO release is associated with the functional groups in these donors.

1. Introduction

Since NO was confirmed that nitric oxide (NO) is the endothelium-derived relaxing factor (EDRF) in 1987 [1], it has been reported to mediate a large number of diverse physiological and pathological processes. On the one hand, it plays an important role in mediating vasoconstriction, signal transmission, apoptosis, immunity and gastrointestinal motility [2]. On the other hand, it associates with the mechanisms of many diseases, including hypertension, central nervous system disorder, gastrelcosis, acute renal failure, septic shock, tumor and so on [3–6]. These findings indicate that NO shows a "contradictory" behavior in these processes depending on its concentration. For example, insufficient NO might lead to hypertension [7]; however, excessive NO would lead to cell death [8]. It was reported that NO generated by inducible nitric oxide synthetase (iNOS) might have harmful effects [9] on ischemia-reperfusion injury, while stimulation of NOS activity in tissues could improve recovery from ischemic damage during transplantation [10]. Thus, to measure NO in biological samples is important for understanding the functions of NO.

The rapid diffusion, high reactivity and short half-life (on the order of seconds) of NO make the detection challengeable [11]. In order to ease this bottleneck in the field of physiologic mechanism research of NO, different strategies based on indirect or direct methods have been proposed, including Griess assay, chemiluminescence, electron spin and paramagnetic resonance spectroscopy, UV–vis spectroscopy, fluorescence and electrochemical methods. NO detection techniques were comprehensively reviewed recently [11]. Electrochemical methods have many advantages, such as small electrode size, low cost, real-time and direct analysis with high sensitivity [6,12]. Based on the literatures, electrochemical methods are the only practical method for NO measurement in real samples [13]. Recently, many types of materials have been applied to NO electrochemical sensor fabrications [14,15]. Due to the effect of small dimension, nanomaterials are largely used as electrocatalysts in NO electrochemical sensors. Gong et al. [16] reported a bifunctional sensor on the basis of hematite nanotubes (HeNTs) embedded in chitosan matrix. It was revealed that the HeNTs distributed in porous-structured chitosan matrix facilitated the oxidation of NO and reduction of O_2 dramatically. Gutierrez et al. [17] elaborated a NO sensor based on the concomitant deposition of single-wall carbon nanotubes (SWNTs) and tetrasulfonated nickel phthalocyanine. After the additional coating of selective membranes, this sensor displayed high sensitivity and good selectivity. He et al. [18] fabricated a biosensor based on nano-alumina film and successfully applied it to the determination of NO released from rat lung. Shim and Lee [19] designed an amperometric NO microsensor based on nanopore-platinized platinum electrode, silanization and an electropolymerized poly-5-amino-1-naphthol (poly-5A1N) film were used to improve selectivity. This sensor was successfully used

* Corresponding author. Tel.: +86 27 68759893; fax: +86 27 68759850.
E-mail address: chenzl@whu.edu.cn (Z. Chen).

0039-9140/$ – see front matter © 2010 Elsevier B.V. All rights reserved.
doi:10.1016/j.talanta.2010.06.035

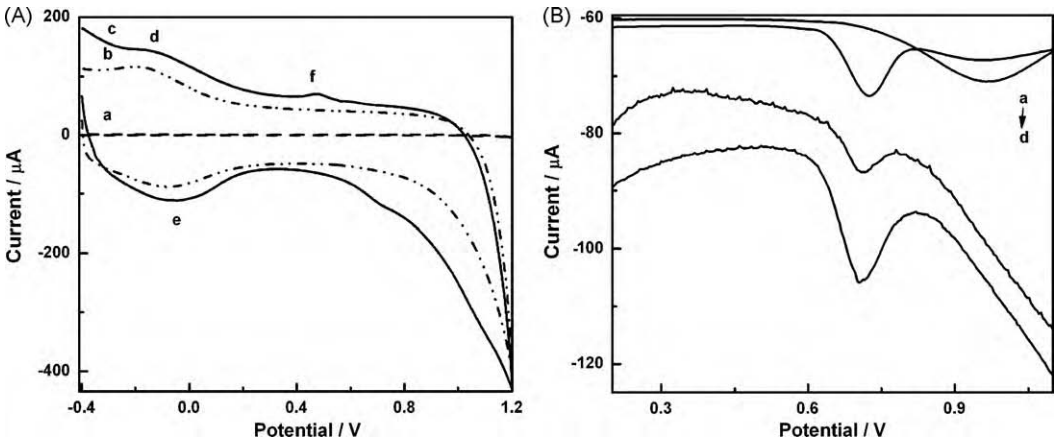

Fig. 1. (A) Electrochemical characterization of (a) bare, (b) MWNTs-CS and (c) MWNTs-CS-AuNPs GCE by CV in 0.01 M PBS (pH 7.4). Scan rate: 0.1 V s^{-1}. (B) DPVs for 3.80×10^{-5} M NO at (a) bare, (b) AuNPs, (c) MWNTs-CS, and (d) MWNTs-CS-AuNPs. Amplitude: 0.05 V, pulse width: 0.05 s.

as a NO-selective probe tip in scanning electrochemical microscopy and obtained a two-dimensional image of the local NO concentration for an inlaid NO-emitting microdisk substrate. Kannan and John [20] described a fused spherical gold nanoparticles-modified ITO electrode, which was highly sensitive and selective towards the oxidation of NO.

Because of the nanometer size, porous structure, good electrocatalytic activities, adsorptive property for biomolecules and minimum surface contamination, MWNTs are of great interest for biosensors. However, the low chemical reactivity and existence in bundles of individual nanotubes of unmodified nanotubes limit their applications [21,22]. The combination of metal nanoparticles and the MWNTs can generate excellent behavior. Considerable reports indicate that high-dispersed nano-size gold particles have catalytic activities, because of their "quantum size effect" [23]. Au nanoparticles (AuNPs) modified electrodes have been successfully used for several kind of bio-samples, such as glucose, SOD, and epinephrine [24–26]. Zhu et al. [27] found that the cysteine and AuNPs based platinum electrode exhibited excellent catalytic activity toward NO. However, linkers like cysteine may reduce the conductivity and the adsorption of AuNPs is still not so enduring. Chitosan (CS) has excellent adhesion capability, film-forming ability, high water permeability and biocompatibility [28]. These properties make it possible to disperse MWNTs well and adsorb Au nanoparticles tightly.

In this work, MWNTs, AuNPs and CS were integrated to improve the sensor sensitivity and capability by synergistic contributions. After further coating with Nafion, this NO sensor revealed good linear relationship for the quantitative analysis of NO. Finally, this NO sensor was applied to the monitoring of NO release from mouse organs including kidney, heart, spleen and liver (a slice) with the stimulation of L-arginine (L-Arg), nitroglycerin (GTN) and aspirin (ASA) as donors.

2. Materials and methods

2.1. Reagents and apparatus

MWNTs (Shenzhen Nanotech Port Co., Ltd., Shenzhen, China) were refluxed in ~12 M nitric acid at 110 °C for 11 h, washed with deionized water to neutral, and then dried at 110 °C for 24 h. AuNPs were prepared as described in Zhu's work [27]. Chitosan (CS) and L-arginine (L-Arg) were obtained from Shanghai Ruji Biological Technology development Co., Ltd. (Shanghai, China). 0.5% Nafion solution was prepared by dilution of 5.0% Nafion (Sigma, USA) with ethanol. Aspirin (ASA) was purchased from Jiangsu Pingguang Pharmaceutical Co., Ltd. (Jiangsu, China), nitroglycerin (GTN) from Beijing Yimin Pharmaceutical Co., Ltd. (Beijing, China). Aqueous solutions were prepared with deionized water (Chongqing Qianyan Water Disposal Equipment Co., Ltd., Chongqing, China). High purity nitrogen (≥99.9%) gas was used for deaeration. Phosphate buffer solution (PBS) was prepared with 7.2 g L^{-1} NaCl, 0.2 g L^{-1} KCl, 1.48 g L^{-1} Na_2HPO_4, 0.4 g L^{-1} KH_2PO_4 and water (pH 7.4). NO stock solution was prepared by a dismutation reaction, in which a concentrated H_2SO_4 solution was used to carry out the disproportion, using $NaNO_2$ as a source of NO_2^- [29]. According to the literature [30], the NO concentration of the saturated aqueous solution is about 1.9 mM. Standard solutions were obtained before each experiment by making a series of dilutions of the NO saturated solution with gas-tight microsyringes.

Electrochemical experiments were performed on a CHI 830 electrochemical workstation (CH Instrument Co., Shanghai, China) at room temperature. A three-electrode system was employed, consisting of a saturated calomel electrode (SCE) as reference electrode, a platinum (Pt) wire (Φ = 0.5 mm) as auxiliary electrode and a modified glassy carbon electrode (GCE) (Φ = 3.0 mm, CHI) as working electrode.

2.2. Preparation of MWNTs-CS-AuNPs/GCE

The MWNTs-CS-AuNPs suspension was prepared in the following procedures: 4.0 mg of purified MWNTs were dispersed in 1 mL of 1.0 mg mL^{-1} CS (in 30 mM acetic acid) with the help of ultrasonic agitation. Then the black solution was mingled with isochoric 3.0-fold enriched gold nanoparticles with the aid of ultrasonic agitation. GCE was polished on a polishing cloth with successively smaller particles (1.0- and 0.05-μm diameter) of Al_2O_3. The slurry on the electrode surface was removed by ultrasonication in deionized water. 10 μL of MWNTs-CS-AuNPs suspension (final concentrations: 2.0 mg mL^{-1} of MWNTs, 0.5 mg mL^{-1} CS and 1.5-fold of AuNPs) was pipetted onto the clean GCE surface, drying in the air.

2.3. Procedures of electrochemical measurement

Differential pulse voltammetry (DPV) was used to study the electrochemical properties of the MWNTs-CS-AuNPs/GCE and evaluate the effect of film thickness. Before NO determination, the prepared sensor was placed in 5 mL of 0.01 M PBS (pH 7.4) and scanned between −0.40 and 1.20 V till steady was observed (usually 20 cycles).

For the amperometric determination of NO, the MWNTs-CS-AuNPs was covered with 2 μL 0.5% Nafion solution and dried in air.

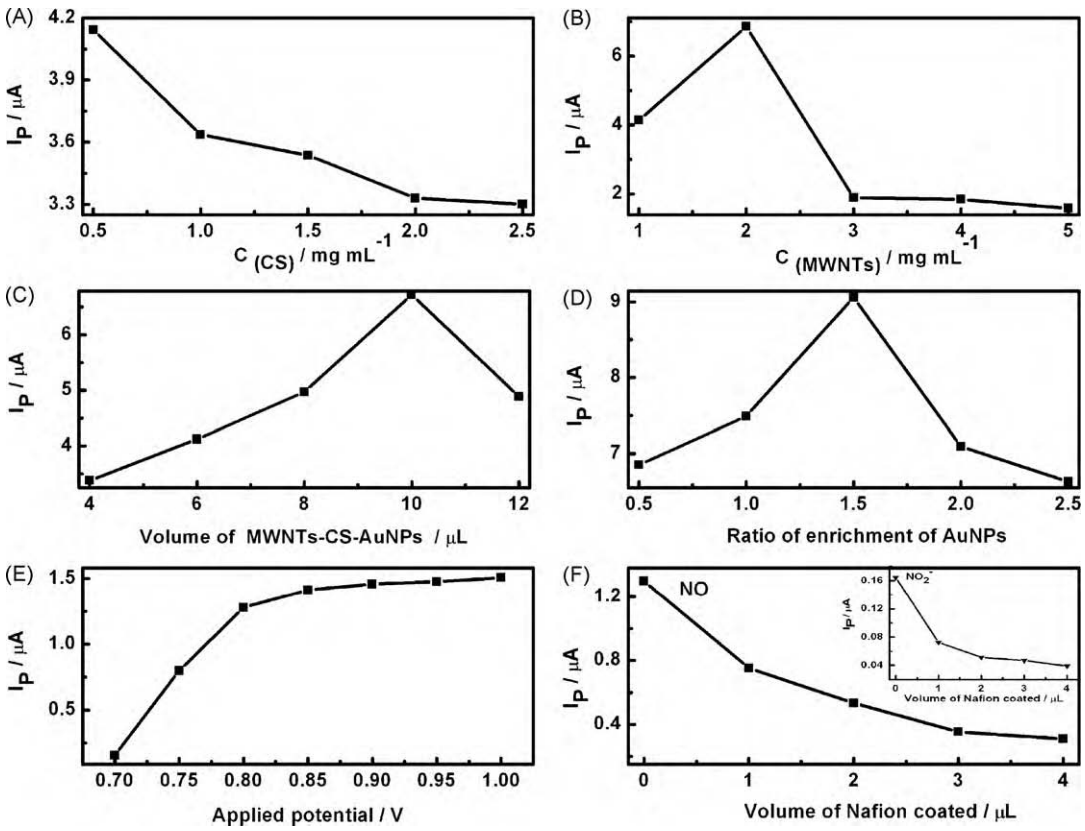

Fig. 2. Effects of concentration of CS (A) and MWNTs (B), amount of MWNTs-CS-AuNPs (C) and quantity of AuNPs (D) on the oxidation peak current by DPV in the presence of 3.80×10^{-6} M NO. Amplitude: 0.05 V, pulse width: 0.05 s. Effect of applied potential (E) and volume of Nafion coating (F) on amperometric determination of NO (3.8×10^{-7} M) and NO_2^- (4.00×10^{-7} M). Applied potential: 0.85 V.

Ampermetry was used to determine the effect of applied potential and volume of Nafion coating, as well as the linearity of the sensor.

2.4. Monitoring of NO release from mouse organs

Male mice were used. Each mouse was sacrificed by decapitation several minutes before determination. Liver, spleen and both kidneys were immediately excised and stored in cold Euro-Collins (32.7 g L^{-1} D-glucose, 2.1 g L^{-1} KH_2PO_4, 7.4 g L^{-1} K_2HPO_4, 1.1 g L^{-1} KCl, and 0.8 g L^{-1} $NaHCO_3$) solution on ice in fridge until they were used for experiments. The heart was prepared in the same way except it was stored in cold Ringer–Lockes solutions (9.0 g L^{-1} NaCl, 0.4 g L^{-1} KCl, 0.5 g L^{-1} $NaHCO_3$, 0.2 g L^{-1} $CaCl_2$, and 1.0 g L^{-1} glucose).

Prior to NO determination, the sensor was scanned potentially between −0.4 and 1.2 V in 1 mL PBS (pH 7.4, unaerated) for 20 segments. Each organ was cleaned with PBS before measurement, and then immersed in the PBS, leaving some part in air. The three-electrode system was positioned into the PBS near the organ as close as possible. Amperometric measurements were started under unstirring conditions. During experiment, L-Arg, GTN and ASA were added into the PBS and the amperometric curve was recorded continuously.

3. Results and discussion

3.1. Electrochemical characterization of different electrodes and their response to NO

Fig. 1A shows the electrochemical behaviors of the electrode modified with different layers in 0.01 M PBS. Compared to the bare GCE (curve a), a couple of redox peaks (peak d and e) on the MWNTs-CS/GCE and MWNTs-CS-AuNPs/GCE (curve b and c) are observed. They are ascribed to the oxidation and subsequent reduction of the functional groups on the surface of MWNTs [31]. In addition, MWNTs can increase the surface area of the electrode dramatically [32], so the background current is much stronger than that of the bare GCE surface. The cathodic peak (peak f, curve c) at 0.47 V is ascribed to the reduction of gold species [33].

Fig. 1B indicates the oxidation of 3.80×10^{-5} M NO at different electrodes. Compare to the bare GCE, the MWNTs-CS-AuNPs/GCE (curve d) can facilitate the oxidation of NO by the negative shift of the oxidation potential from 0.96 (curve a) to 0.71 V. Both AuNPs/GCE and MWNTs-CS/GCE can also negatively shift the oxidation potential of NO (curve b and c). Besides, the MWNTs-CS-AuNPs/GCE can get larger oxidation current than AuNPs/GCE or MWNTs-CS/GCE does. It indicated that the combination of AuNPs and MWNTs-CS shows better electrocatalytic activity. When MWNTs-CS is coated on the GCE surface, the oxidation of NO is catalyzed and the peak potential shift negatively. The reason may be that the excellent conductivity and particular space constructure of carbon nanotubes make the electron transfer easy [31]. Due to the excellent film-forming ability, CS enables to distribute MWNTs on the surface of electrode very well. After AuNPs is added, the peak currents increased largely. This phenomenon results from the synergistic effect of AuNPs and CS. AuNPs can work as tiny "electrons antennae" [34], while CS binds AuNPs tightly on the electrode surface.

3.2. Optimization of experimental parameters

3.2.1. Optimization of parameters related to film thickness

CS has been well studied [35,36]. It is a linear polysaccharide having excellent membrane-forming ability, adhesion capabil-

ity, high mechanical strength, and high permeability towards water, non-toxicity and good biocompatibility [36,37]. However, CS has poor electrical conductivity and it would block electrons transfer. Thus, the optimization of the amount of CS is important for the electrochemical determination of NO. Fig. 2A shows the relationship between the peak current of NO oxidation and the concentration of CS. Based on the experimental results, a balance between forming-film and electron transfer-hampering could be obtained when 0.5 mg mL^{-1} chitosan was used.

MWNTs treated by oxidation produce various functional groups such as hydroxyl and carboxyl. Both the walls and the defect sites at the ends of the nanotubes have electrochemical properties [31]. Moreover, MWNTs can offer sensors with a large surface area. Therefore, MWNTs possess an attractive property of "elecrocatalysis". Fig. 2B shows the effect of MWNTs concentration on the peak current of NO oxidation. The largest peak current can be obtained at 2.0 mg mL^{-1} of MWNTs modified electrode. It can be explained as follows: MWNTs are randomly distributed onto the GCE surface. This distribution can enlarge the surface area. However, excessive MWNTs may accumulate and form a thick MWNTs film, hindering the electron transfer. The influence of the volume of MWNTs-AuNPs suspension (Fig. 2C) can be explained in the same way and 10 μL of the suspension volume was preferable.

AuNPs are faradaically inactive and the electron transfer occurs directly at the AuNPs/solution interface so that these small particles could efficiently funneling electrons between the electrolyte and the electrode [34,38]. AuNPs have high surface-to-volume ratio and the catalytic properties of transition metal. However, excessive nanoparticles will aggregate together and nano-size turns into micro-size or even larger, and the catalytic activity of AuNPs would attenuate. Fig. 2D shows the effect of the ratio of enrichment of AuNPs on NO oxidation current. The electrode modified with 1.5-fold enriched gold nanoparticles can produce the maximum peak current.

3.2.2. Applied potential

Fig. 2E shows the influence of the applied potential on the amperometric response of NO. The oxidation current increases sharply in the potential range from 0.70 to 0.80 V, and then increases slowly after 0.85 V. However, background current will significantly increase at higher potentials. Many electroactive components may also be oxidized under high potential. Consequently, the optimum potential for NO amperometric detection was selected at 0.85 V vs. SCE.

3.2.3. Amount of Nafion

For detection of NO in real samples at high potentials, Nafion, a cation-exchange film was chosen to enhance the selectivity of nitric oxide sensor. It cannot only act as a barrier to discriminate against anions, but also prevents the electrode from contamination due to the non-specific adsorption of proteins and other materials [39]. However, the Nafion membrane will lower the sensitivity of the sensor. Therefore, for the best balance between selectivity and sensitivity, optimization of amount of Nafion is important. Fig. 2F shows the effect of volume of Nafion on the response of NO and NO_2^-. As observed in Fig. 2F, the NO response current decreased to 57.9% of the initial response after 1 μL 0.5% Nafion was coated onto the MWNTs-CS-AuNPs/GCE surface, while the NO_2^- response decreased to 44.1%. This result illustrated that Nafion can improve the selectivity of the NO sensor. Besides, the response of NO_2^- decreased slightly when 2 μL or more Nafion was coated. Therefore, 2 μL 0.5% Nafion coated on the MWNTs-CS-AuNPs/GCE was chosen to prepare the sensor.

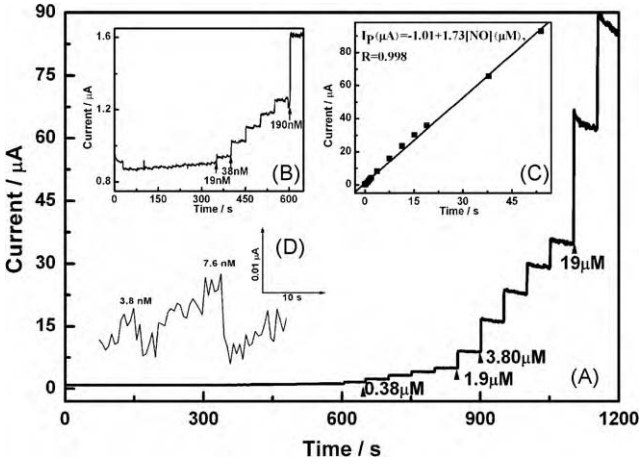

Fig. 3. Amperogram (A) at the sensor with successive injections of different concentrations of NO in PBS. Inset graph (B), the amplificatory image of amperometric response from 0 s to 600 s. Inset graph (C) shows the corresponding calibration plot. Inset graph (D) shows the detection limit. Applied potential: 0.85 V.

3.3. Amperometric detection of NO

NO is easily oxidized to nitrite, so response time is a critical parameter for sensors evaluation. Our NO sensor showed a rapid response that the 90% response time for a step from 0 to 3.80 μM NO is about 4 s.

The calibration curve of NO assay with this sensor was plotted, as shown in Fig. 3A, the linear relationship between NO concentrations and the oxidation currents is in a range of 1.90×10^{-8} to 5.40×10^{-5} M. The equation can be stated as I_P (μA) = −1.01 + 1.73[NO] (μM) with a correlation coefficient $R = 0.998$ (Fig. 3C). The sensitivity of the NO sensor was 1.73 μA μM^{-1} and the detection limit was estimated to be 7.60×10^{-9} M (Fig. 3D, the signal-to-noise ratio is 3).

3.4. Selectivity, stability and reproducibility

The possible interfering species from other electroactive species in biological samples have been tested. The results showed that 1.50×10^{-2} M glucose, 3.00×10^{-4} M L-Arg, 1.70×10^{-4} M DA, 1.20×10^{-4} M UA, 3.00×10^{-5} M AA, 2.00×10^{-5} M $NaNO_2$, and 1.25×10^{-5} M L-Cys almost had no interference with the determination of 3.80×10^{-6} M NO. Some major metal ions in biological samples like Ca^{2+}, Mg^{2+}, Fe^{3+} and Zn^{2+} were also examined. Several hundreds folds of these cations can hardly interfere with the NO determination (signal change less than 8.0%).

The stability and reproducibility were also investigated. Stability remained 93.0% of its initial response after 8 days. Eight separately prepared sensors were used for the reproducibility test and the oxidation peak currents were the same for detection of 1.90×10^{-5} M NO with a relative standard deviation (RSD) of 4.7%. It suggests that the sensor has good reproducibility.

The sensor performance was compared with commercially available and recently reported NO sensors. As summarized in Table 1, the sensor possesses comparable capability with others.

3.5. Monitoring NO released from rat organs

Nitric oxide plays a major role in controlling nearly every cellular and organ function in the body [6]. Previous reports show that NO is biosynthesized from L-Arg in the presence of NOS [51], from GTN in the presence of enzymes such as cytochrome p450 enzymes or xanthine oxidoreductase [52] or from ASA due to a direct acetylation of the NOs protein [53]. NO induced by L-Arg from kidney [54],

Table 1
Comparison of sensitivity, detection limits and dynamic range with different NO sensors.

Electrode	Modifiers	Sensitivity	Detection limit (nM)	Dynamic range (M)	Ref.
CF[a] (Φ[b] = 100 μm)	Nafion/WPI memberane	n.r.[c]	0.5	6.75×10^{-10} to 1.35×10^{-8}	[40]
CF (Φ = 7 μm, l[d] = 2 mm)	Nafion/WPI memberane	0.5–2.0 pA/nM	5	1.0×10^{-8} to 5.0×10^{-6}	[41]
CF (Φ = 0.1 μm, l = 150 μm)	Nafion/WPI memberane	0.1–1.0 pA/nM	2	1.0×10^{-8} to 1.0×10^{-6}	[42]
MC[e] (3 × 5 mm)	Nafion/WPI memberane	~17 pA/nM	0.3	1.0×10^{-9} to 5.0×10^{-5}	[43]
PtD[f] (Φ = 200 μm)	Nafion/Au_{nano}/Cysteine	n.r.	50	1.0×10^{-7} to 4.0×10^{-5}	[27]
PtD (Φ = 25 μm)	Poly-5A1N	122.0 ± 2.5 pA/μM	5.8	2.0×10^{-7} to 1.8×10^{-6}	[44]
PtW[g] (Φ = 125 μm)	CS/*o*-PD/MB	20 nA/μM	1	1.0×10^{-8} to 6.0×10^{-4}	[45]
GC[h] (Φ = 3.0 mm)	4α-Co^{II}TAPc	n.r.	0.14	3.0×10^{-9} to 3.0×10^{-8}	[46]
GC (Φ = 3.0 mm)	Nafion/MWNTs	n.r.	80	2.0×10^{-7} to 1.5×10^{-4}	[32]
GC (Φ = 3.0 mm)	Nafion/MWNTs-ACB/PACB	0.25 μA/μM	28	2.2×10^{-7} to 1.2×10^{-4}	[47]
GC (Φ = 3.0 mm)	Au_{mf}/Au_{bf}	n.r.	27	5.0×10^{-8} to 1.0×10^{-5}	[33]
GC (Φ = 3.0 mm)	PPV derivative	42.68 nA/μM	23	1.8×10^{-7} to 1.0×10^{-4}	[48]
GC (Φ = 3.0 mm)	Cyc c/SDS/PAM	n.r.	100	8.0×10^{-7} to 9.5×10^{-5}	[49]
GC (Φ = 3.0 mm)	PEB-IL	n.r.	18	3.6×10^{-8} to 1.3×10^{-4}	[50]
GC (Φ = 3.0 mm)	Nafion/MWNTs-CS-AuNPS	1.73 μA/μM	7.6	1.9×10^{-8} to 5.4×10^{-5}	This work

[a] CF, carbon fiber;
[b] Φ, diameter;
[c] n.r., not refer;
[d] l, length;
[e] MC, microchip,
[f] PtD, platinum disk,
[g] PtW, platinum wire;
[h] GC, glassy carbon.

heart [38], liver [55] and other tissues [56–58] have been measured by different electrodes. In this work, NO releases stimulated by L-Arg, GTN and ASA from four mouse organs (kidney, heart, spleen and liver) were investigated.

Take the kidney stimulated by L-Arg as an example, no current response appears without kidney or L-Arg in the PBS (Fig. 4A: curve a–c). However, when 5.00 mM of L-Arg was added into the PBS immersing kidney, an amperomeric response was observed after 30 s. The highest response was obtained about 380 s later (curve d). The result suggests that the amperomeric signal changes presented in the figure are due to the variations of NO generation from the kidney induced by the addition of the L-Arg.

We have also tested the amperometric response of NO release from different living organs stimulated by successive addition of L-Arg, GTN and ASA. As indicated in Fig. 4B, it is observed that oxidation currents of NO released from kidney, heart, spleen and liver (a slice) are not the same after successive stimulation with L-Arg. These results reflect that the activities and tolerances of NOS in these organs are probably different. The oxidation currents and relevant NO concentrations are listed in Table 2. Besides, when converting the three stimulants to the same concentration, ASA could induce more NO than L-Arg did and GTN could induce the largest increase in NO generation. It was interestingly inferred that the NO release from organs was associated with their chemical structures of the drugs used for stimulation. As shown in Fig. 5, there are three nitryl groups in GTN, one imino group in L-Arg, no nitrogen group but an acetyl group in ASA. It is inferred that GTN can induce more NO because two of the nitryl groups can produce NO [59], ASA can induce more NO because the acetyl group can acetylate NOS directly [53]; however, L-Arg requires two steps to produce NO [51]. Furthermore, the stronger hydrophobicity of the GTN also facilitates its passive transport into the cells within the organs.

In fact, it needs to be declared that the way of stimulation, the sensor location, the living organ activity and physiologic factors associated with the mouse would affect the measured NO level, because of different diffusion distances, different enzyme synthesis capacities, degradation of NO by active dissolved oxygen, oxyhemoglobin and various reactive species present in the living organs. However, it is the first time to measure NO release from four mouse organs simultaneously by electrochemical sensor and to reveal

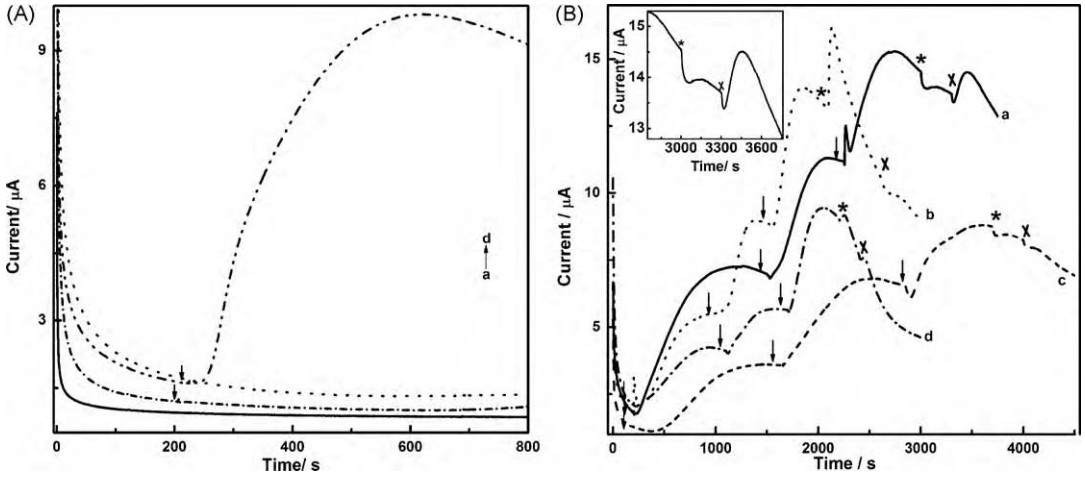

Fig. 4. (A) Amperograms at the sensor (a and b) in the absence or (c and d) presence of mouse kidney when adding (a and c) 0, (b and d) 5.00 mM L-Arg. (B) Amperograms in the presence of rat kidney (a), heart (b), spleen (c) and liver (a slice, d) by adding 5.00 mM L-Arg., 13.60 μM GTN and 0.70 mM ASA as donors at the position symbols directed. Inset shows the amplificatory image of stimulating kidney with GTN and ASA ("↓" L-Arg "*" GTN, "×" ASA). Applied potential: 0.85 V.

Table 2
NO release from four mouse organs in the presence of L-Arg, GTN and ASA.

Organs	L-Arg (5.00 mM)	L-Arg (5.00 mM)	L-Arg (5.00 mM)	GTN (13.60 μM)	ASA (0.70 mM)
Kidney	5.59[a] (3.82)[b]	4.55 (3.21)	3.79 (2.77)	0.11 (0.65)	1.16 (1.25)
Heart	3.43 (2.57)	3.46 (2.58)	5.35 (3.68)	–[c]	0.08 (0.63)
Spleen	2.53 (2.05)	3.31 (2.50)	2.74 (2.17)	0.10 (0.64)	0.07 (0.62)
Liver (a slice)	2.21 (1.86)	1.65 (1.54)	3.90 (2.84)	0.20 (0.70)	0.11 (0.65)

[a] Amperometric currents (μA) from NO upon stimulation with L-Arg, GTN and ASA (according to Fig. 4B).
[b] NO concentrations (μM) scalered from the calibration equation.
[c] Data unable to be read from Fig. 4B.

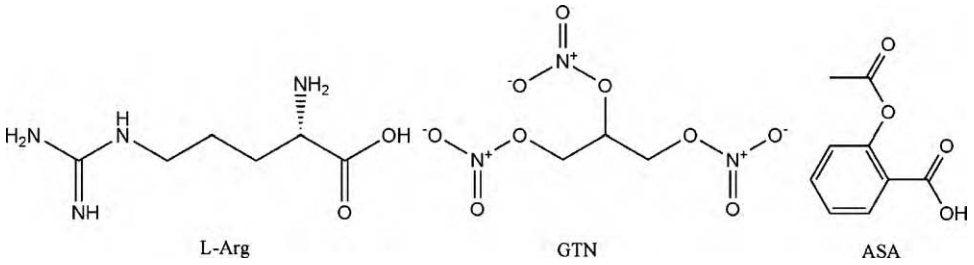

Fig. 5. Chemical structures of L-Arg, GTN and ASA.

the differences in three NO donors with different chemical structures. Hopefully, the results in this work could provide scientific evidence for scientists who work on NO release and pathological mechanisms.

4. Conclusions

A nitric oxide sensor based on Nafion/MWNTs-CS-AuNPs/GCE has been developed successfully in this work. The sensor has many merits such as fast response time, favorable stability and reproducibility. The amperometric current is proportional to the concentration of NO over a broad range with a low detection limit. Moreover, the sensor was successfully applied to monitoring NO released from mouse organs stimulated with L-Arg, GTN and ASA. Response currents obtained from successive stimulation with L-Arg were diverse and NO release from four organs displayed different behaviors. It was interestingly found that the amount of NO release was related to the chemical groups that NO donors provide. GTN could induce more NO release than ASA or L-Arg does, probably because of the three nitryl groups in GTN and its stronger hydrophobicity. These preliminary results suggest that this sensor responds to changes of NO in the organs of mouse. Optimistically, the sensor shows great application potential in NO-related studies such as mechanisms of drug interaction, physiological and pathological mechanisms and signaling pathway.

Acknowledgements

This work was supported by the Fundamental Research Funds for the Central Universities and the start-up fund for Luojia Chair Professorship of Wuhan University (No. 306276216 and 306271159), the National Scientific Foundation of China (NSFC NOs. 20775055, 30973672, 90817103 and 6080102.0), the Important National Science & Technology Specific Projects (No. 2009ZX09301-14).

References

[1] R.M.J. Palmer, A.G. Ferrige, S. Moncada, Nature 327 (1987) 524.
[2] M. Maskus, F. Pariente, Q. Wu, A. Toffanin, J.P. Shapleigh, H.D. Abrunna, Anal. Chem. 68 (1996) 3128.
[3] M.S. Goligorsky, S.V. Brodsky, E. Noiri, Kidney Int. 61 (2002) 855.
[4] W.H. Kan, K.S. Zhao, Y. Jiang, W.S. Yan, Q.B. Huang, J.Z. Wang, Q.H. Qin, X.L. Huang, S.W. Wang, Shock 21 (2004) 281.
[5] J.R. Lancaster, K.P. Xie, Cancer Res. 66 (2006) 6459.
[6] Z.H. Taha, Talanta 61 (2003) 3.
[7] R. Lapu-Bula, E. Ofili, Am. J. Cardiol. 99 (2007) S7.
[8] L. Bosca, S. Hortelano, Cell. Signal. 11 (1999) 239.
[9] I.H.C. Vos, J.A. Joles, M. Schurink, G. Weckbecker, T. Stojanovic, T.J. Rabelink, H.J. Gröne, Eur. J. Pharmacol. 391 (2000) 31.
[10] E.L. Rhoden, L. Pereira-Lima, C.R. Rhoden, M.L. Lucas, C. Telöken, A. Belló-Klein, Eur. J. Surg. 167 (2001) 224.
[11] E.M. Hetrick, M.H. Schoenfisch, Annu. Rev. Anal. Chem. 2 (2009) 409.
[12] Y. Lee, J. Kim, Anal. Chem. 79 (2007) 7669.
[13] S. Griveau, J. Seguin, D. Scherman, G.G. Chabot, F. Bedioui, Electroanalysis 21 (2009) 631.
[14] A. Ciszewski, G. Milczarek, Talanta 61 (2003) 11.
[15] C.N. Hall, J. Garthwaite, Nitric Oxide 21 (2009) 92.
[16] J.M. Gong, L.Y. Wang, K. Zhao, D.D. Song, L.Z. Zhang, Electrochem. Commun. 10 (2008) 1222.
[17] A.P. Gutierrez, S. Griveau, C. Richard, A. Pailleret, S.G. Granados, F. Bedioui, Electroanalysis 21 (2009) 2303.
[18] Q. He, D.Y. Zheng, S.S. Hu, Microchim. Acta 164 (2009) 459.
[19] J.H. Shim, Y. Lee, Anal. Chem. 81 (2009) 8571.
[20] P. Kannan, S.A. John, Electrochim. Acta 55 (2010) 3497.
[21] G. Mestl, N.I. Maksimova, N. Keller, V.V. Roddatis, R. Schlögl, Angew. Chem. Int. Ed. 40 (2001) 2066.
[22] P. Serp, M. Corrias, P. Kalck, Appl. Catal. A 253 (2003) 337.
[23] S.H. Overbury, V. Schwartz, D.R. Mullim, W.F. Yan, S. Dai, J. Catal. 241 (2006) 56.
[24] D. Feng, F. Wang, Z.L. Chen, Sens. Actuators, B 138 (2009) 539.
[25] Z.Y. Lin, L.Z. Huang, Y. Liu, J.M. Lin, Y.W. Chi, G.N. Chen, Electrochem. Commun. 10 (2008) 1708.
[26] Z.S. Yang, G.Z. Hu, X. Chen, J. Zhao, G.C. Zhao, Colloids Surf. B 54 (2007) 230.
[27] M. Zhu, M. Liu, G.Y. Shi, F. Xu, X.Y. Ye, J.S. Chen, L.T. Jin, J.Y. Jin, Anal. Chim. Acta 455 (2002) 199.
[28] T. Klotzbach, M. Watt, Y. Ansari, S.D. Minteer, J. Membr. Sci. 282 (2006) 276.
[29] J.N. Younathan, K.S. Wood, T.J. Meyer, Inorg. Chem. 31 (1992) 3280.
[30] I.G. Zacharia, W.M. Deen, Ann. Biomed. Eng. 33 (2005) 214.
[31] D. Vairavapandian, P. Vichchulada, M.D. Lay, Anal. Chim. Acta 626 (2008) 119.
[32] F.H. Wu, G.C. Zhao, X.W. Wei, Electrochem. Commun. 4 (2002) 690.
[33] Y.J. Li, C. Liu, M.H. Yang, Y. He, E.S. Yeung, J. Electroanal. Chem. 622 (2008) 103.
[34] K.C. Grabar, R.G. Freeman, M.B. Hommer, M.J. Natan, Anal. Chem. 67 (1995) 735.
[35] Y.A. Shchipunov, T.Y. Karpenko, Langmuir 20 (2004) 3882.
[36] V. Pedroni, P.C. Schulz, M.E.G. de Ferreira, M.A. Morini, Colloid Polym. Sci. 278 (2000) 964.
[37] V.V. Binsu, R.K. Nagarale, V.K. Shahi, React. Funct. Polym. 66 (2006) 1619.
[38] K.R. Brown, A.P. Fox, M.J. Natan, J. Am. Chem. Soc. 118 (1996) 1154.
[39] G.A. Gerhardt, A.F. Oke, G. Nagy, B. Moghaddam, R.N. Adams, Brain Res. 290 (1984) 390.
[40] K.J. Mantione, G.B. Stefano, Med. Sci. Monit. 10 (2004) MT49.
[41] X.J. Zhang, L. Cardosa, M. Broderick, H. Fein, J. Lin, Electroanalysis 12 (2000) 1113.
[42] X.J. Zhang, Y. Kislyak, H. Lin, A. Dickson, L. Cardosa, M. Broderick, H. Fein, Electrochem. Commun. 4 (2002) 11.
[43] X.J. Zhang, J. Lin, L. Cardoso, M. Broderick, V. Darley-Usmar, Electroanalysis 14 (2002) 697.
[44] J.H. Shim, H. Do, Y. Lee, Electroanalysis 22 (2010) 359.
[45] J. Njagi, J.S. Erlichman, J.W. Aston, J.C. Leiter, S. Andreescu, Sens. Actuators, B 143 (2010) 673.

[46] A. Sivanesan, S.A. John, Electroanalysis 22 (2010) 639.
[47] D.Y. Zheng, C.G. Hu, Y.F. Peng, W.Q. Yue, S.S. Hu, Electrochem. Commun. 10 (2008) 90.
[48] Y.Z. Wang, S.S. Hu, Bioelectrochemistry 74 (2009) 301.
[49] X. Chen, H.Y. Long, W.L. Wu, Z.S. Yang, Thin Solid Films 517 (2009) 2787.
[50] Y.F. Peng, Y.P. Ji, D.Y. Zheng, S.S. Hu, Sens. Actuators, B 137 (2009) 656.
[51] R.M.J. Palmer, D.S. Ashton, S. Moncada, Nature 333 (1988) 664.
[52] Y. Minamiyama, S. Takemura, T. Akiyama, S. Imaoka, M. Inoue, Y. Funae, S. Okada, FEBS Lett. 452 (1999) 165.
[53] D. Taubert, R. Berkels, N. Grosser, H. Schroder, D. Grundemann, E. Schomig, Br. J. Pharmacol. 143 (2004) 159.
[54] Y. Lee, J. Yang, S.M. Rudich, R.J. Schreiner, M.E. Meyerhoff, Anal. Chem. 76 (2004) 545.
[55] Y.Z. Wang, S.S. Hu, Biosens. Bioelectron. 22 (2006) 10.
[56] F.Y. Du, W.H. Huang, Y.X. Shi, Z.L. Wang, J.K. Cheng, Biosens. Bioelectron. 24 (2008) 415.
[57] R. Hernanz, M.J. Alonso, H. Zibrandtsen, Y. Alvarez, M. Salaices, U. Simonsen, Cardiovasc. Res. 62 (2004) 202.
[58] W.C. Wu, Y. Wang, L.S. Kao, F.I. Tang, C.Y. Chai, Brain Res. Bull. 57 (2002) 171.
[59] K. Lange, A. Koenig, C. Roegler, A. Seeling, J. Lehmann, Bioorg. Med. Chem. Lett. 19 (2009) 3141.